Slow scan SEC vidicon system

Hong-Yee Chiu

A slow scan SEC vidicon system is described here. This system is coupled to the 152.4-cm (60-in) McMath telescope at Kitt Peak National Observatory. An anamorphic lens system is used to couple optically the vertical spectrograph to the vidicon system. The resolution of the over-all system is 55 mÅ, while the resolution of the spectrograph alone is 50 mÅ. Actual observational results are used to evaluate the system performance.

I. Introduction

The use of electronic imaging devices to integrate low level light signals has gained popularity in astronomy in recent years. In particular, sensitive SEC tubes capable of long integration times have been developed and applied to astronomical work. In the early work with such detectors, a number of problems hindered this application, such as nonuniform landing of the electron beam on the target and the presence of residual images. However, these drawbacks are now overcome by improved operational procedures. Quantitative results with 1% accuracy have been reported, and in a single exposure, accuracies better than 5% can be obtained. In this paper we report an experimental slow scan, integrating TV system using the Westinghouse WX-31958 SEC tube as the detector. This vidicon system is designed to register accurately low level signals for use in astronomical observations.

In Sec. II we present technical details of the system. In Sec. III the adaptation of this system to the vertical spectrograph of the 152.4-cm (60-in) McMath solar telescope for observations of stellar spectra at high dispersion is described. In Sec. IV, we discuss the anamorphic optical transfer system that matches the spectrographic image to the vidicon format. In Sec. V, some observational results are discussed in an evaluation of the performance of the system. In Sec. VI, we discuss various problems encountered in practical operation of a SEC vidicon system at the telescope.

II. Technical Details of the SEC Vidicon System

The principle of SEC vidicon and its operation have been discussed previously by other authors.[1–4] The Westinghouse WX-31958 SEC vidicon has a magnetically focused photocathode image section. This photocathode operates at a nominal potential of 7.4 kV relative to the target. The target is composed of low density KCl and has an active area of 2.5 cm × 2.5 cm. The useful operational voltage range of the target is somewhat below 15 V at a gain of around 50.

In low level light applications, the SEC vidicon suffers from contamination by latent images from previous exposures and from nonuniform beam landing in low light areas of the target. To overcome these two problems, standardized sequences of operational procedures have been developed by various researchers. The operational procedures we adopted in this system to initiate an exposure and readout sequence include the following stages: (1) erasure of residual images due to previous exposures; (2) target preparation; (3) exposure by application of proper photocathode potentials; (4) readout of signals.

At stage (1), the target potential is lowered by several volts, and the electron beam is defocused during subsequent scans. After a delay time required for various internal tube potentials to achieve equilibrium, light of sufficient intensity to saturate the target is applied with the photocathode at its operational potential. A series of rapid scans then takes place to remove the saturated signals. During stage (2), the electron gun focusing fields are restored, and the target potential is raised to a fraction of 1 V, ΔV below that is imposed at the readout stage (4). The target is then scanned several times to ensure proper charging. The value of ΔV depends on the particular setup but generally lies between 0.3 V and 0.6 V. This increase in the target voltage at stage (4) is necessary due to the thermal energy spread (~0.3 eV) of the electrons in the scanning beam. Raising the target voltages by ΔV insures that sufficient electrons can always land. Although this practice tends to increase the background noise by a small amount, the advantage of a uniform beam landing outweighs other problems.

The author is with NASA Goddard Institute for Space Studies, New York, New York 10025.

Received 29 May 1976.

Table I. Operational Steps of SEC Vidicon System

Function	Erase								Target Preparation					Exposure		Read out
Step	1	2	3	4	5	6	7	8	9	10	11	12	13	14	15	16
Program																
Scan rate/beam int.[a]	*F*											*F*	*Slo*	*x*	*x*	*Slo*
Scan status[b]	*Sc*												*Sc*	no	no	*M*
Scan size[c]	*O*				*O*	*N*							*N*	*x*	*x*	*N*
Scan beam	Off	On				On	Off	Off	On				On	Off	Off	On
Scan beam focusing[d]	→*L*	*L*					*L*	→*H*	*H*							*H*
Photocathode	Off	On	On	On	Off								Off	*M*	Off	Off
Erase light	Off	On	On	On	Off											Off
Target potential[e]	→*L*	*L*					*L*	→*Med*	*Med*				*Med*	→*H*	*H*	*H*
System status[b]	*R*												*R*	*M*	*M*	*M*

[a] *F* = fast scan and high beam intensity, *Slo* = slow scan and low beam intensity, *x* = irrelevant.
[b] *Sc* = scan starts automatically, *M* = manual start.
[c] *O* = over scan, *N* = normal scan.
[d] Scan beam focusing is controlled by EG3/EG4. At low (*L*) fields focusing is absent, at high (*H*) fields focusing is present.
[e] Voltage between high (*H*) and medium (*Med*) is ΔV = 0.3–0.6 V, between medium (*Med*) and low (*L*) is 2–3 V. Nominally the voltage at high state is 10–12 V.
[d] *R* = automatic cycling, *M* = manually controlled cycling.

In our system the four stages of operation consists of sixteen operational steps which are outlined in Table I. Fine divisions of the four stages into various steps are somewhat arbitrary, depending on individual needs and operational conditions. In the current system the sequential steps are executed automatically by a hard-wired sequencer device. Admittedly a minicomputer might be a better choice for programming versatility. However, once the proper sequence is determined, a hard-wired sequencer has the advantage of being lightweight, of lower cost, and more dependable. Our apparatus was constructed before microprogrammer technology became commercially available.

The readout of the signal is accomplished with an analog (continuous) line scan and a digital (stepped) frame scan. Continuous line scan is used in order to simplify design problems involved in the pulsed-beam mode operation. As each line is scanned, the signal is sampled and digitized at 1024 equally spaced intervals. The digital data (twelve-bit resolution) are then stored in a buffer memory and transferred to a digital tape recorder. After the signals from each line have been processed, another line scan takes place and so on.

The line scan and frame scan ramp signals are generated from a crystal-controlled clock signal. In the slow scan mode, the line scan period is 16.7 msec (the corresponding frequency is 60 Hz), and the start of each line scan is synchronized to a zero-crossing point of the 60-Hz ac power. We found this synchronization to be necessary in order to avoid amplification of small contaminating ac signals in the circuits, especially when a digital tape recorder is used to record the signals, since the recording speed of most tape recorders is slower than the direct readout speed of the system, and interference can easily result from out-of-phase noise from the ac line.

The clock frequency is 61,440 Hz in the slow scan mode. This frequency is the same as that in the Princeton system[3,4] and has been chosen to be a compromise between the $1/f$ shot noise and the Johnson noise ($\sim \sqrt{f}$). In most operations we choose a raster scan consisting of 740 lines. This choice is for convenience in our applications; it should be noted that Lowrance and Zucchino reported that a properly chosen set of deflection coils can give sufficient resolution at a 1000 line raster.

The line scan and frame scan ramp signals are generated from clock signals, using D/A converters. The line ramp signal is derived from a ten-bit D/A converter. The frequency response of the deflection amplifier tends to smooth out the irregularities inherent in the bit-to-bit stepping transitions. However, in the frame scan we found that this irregularity tends to yield signals of uneven strength. To remedy this, a sixteen-bit D/A converter is used to provide an accurate ramp. The bit-to-bit irregularity is reduced by a factor of 2^{-6}.

The preamplifier consists of an input stage using a selected Teledyne Philbrick AM 101B FET operational amplifier with a feedback resistor of 5000 MΩ. After initial warmup, this amplifier appears to be quite stable in gain, and the noise is roughly 5 pA at 20 kHz. At a target gain of 50, this corresponds to sixteen photoelectrons per pixel. This is not the most optimum choice for a preamplifier design but is a convenient one to use.

In order to provide on-site data evaluation capability, a tape read unit is incorporated so that video signals from any line scan can be displayed or plotted in a plotter. Furthermore, an Alden model 9279A printer has been adapted to the system so that medium quality halftone prints can be obtained immediately after an exposure. In some applications we have also made use of a digital scan converter developed at Kitt Peak National Observatory by P. R. Vokac.

III. Coupling of the Vidicon System to McMath Telescope

Although this vidicon system can be adapted to any telescope capable of sustaining the weight of the camera head (~20 kg), we have used it most frequently with the vertical spectrograph of the 152-cm (60-in.) McMath solar telescope at Kitt Peak National Observatory.

The McMath telescope was constructed in the early 1960's.[5] The design function was to observe the sun with the highest spectral resolution. The main spectrograph provides a high resolution: at the seventh grating order, the dispersion is 11 mm/Å at the photographic port, and a resolution (full width at half-maximum) of 50 mÅ (0.55 mm in linear scale) actually has been achieved both by photographic users and in our work.

The primary mirror of this telescope has a long focal ratio at *f*:56. In order to use it efficiently for stellar observations, an image slicer is provided for use with the main spectrograph. The resulting image of the spectrum of a star assumes a finite height of 2 cm at the photographic port, and at a resolution of 50 mÅ the corresponding linear dimension of a resolvable element is 0.55 mm. The linear dimension of a pixel in our system is 0.025 mm (25 μm), and the typical MTF of the SEC vidicon at 1000 TV line resolution is around 50%. In order to match the resolution of the spectrograph and to provide a sufficient wavelength coverage, we chose a reduction factor of 5:1 which gives a scale factor of 0.11 mm for a resolution of 50 mÅ. Thus, a line of infinitely narrow bandwidth will have a full width at half-maximum of 4 pixels. At this reduction factor, a total of 14 Å can in principle be covered by the 2.5-cm target. However, we decided to avoid the edges of the target and choose a total wavelength coverage of around 9 Å, which is largely determined by the size of the field lens (10-cm diam) used in the transfer optics system. The area covered in the image of the spectrum at the photographic port is roughly 10 cm along the direction of dispersion (horizontal direction) by 2 cm in the perpendicular direction. A simple reduction by using spherical transfer optics will then yield a 2-cm × 0.4-cm image. If the direction of dispersion is aligned along the scanning raster, the 2-cm × 0.4-cm image will correspond to 120 scanning lines, each of these lines carrying the same information. Let N be the total number of photons carrying identical information falling onto the corresponding pixels in the m lines. Let the readout electronic noise be p per pixel. Then the total noise is $\sqrt{N + mp}$, giving a SNR

$$s/n = N/(\sqrt{N + mp}).$$

Thus, decreasing the number of lines covered by the spectrum (i.e., concentrating the spectrum to a lesser number of lines) increases the SNR until $\sqrt{N} \gtrsim mp$. On the other hand, because of target blemishes and other noise considerations, it is also desirable that the identical information be spread to as many lines as possible. We finally choose, for practical reasons, a value of 14 for m. This value of m gives $\sqrt{N} \sim mp$, assuming that the number of photoelectrons per pixel is 1000 (around half of the saturation value) and a readout noise of around 16 photoelectrons per pixel.

We therefore need a transfer optics system with a horizontal reduction factor of 5 and a vertical reduction factor of 43. One such system has been designed and fabricated by us, and this system will be discussed fully in the next section. It may be pointed out that since the reimaging optics of the spectrograph has a focal ratio of 56, the image output of our transfer optics effectively has a focal ratio of 12 in the dispersion direction and a focal ratio of only 1.4 in the perpendicular direction.

The entire vidicon setup at the spectrograph tank is shown in Fig. 1. The optics are aligned with a laser beam with the telescope mirrors adjusted to the autocollimation position. This autocollimation mode also allows the use of standard lamps for relative and absolute intensity calibrations, an advantage that is not available in many other telescopes.

IV. Anamorphic Transfer Optics

The transfer optics mentioned in Sec. III consists of cylindrical and spherical lenses and is capable of reimaging the primary image from the photographic port with orthogonal reduction ratios of 5:1 × 43:1. The optical schematic is shown in Fig. 2. L_1 is a negative cylindrical lens of focal length f_1, L_2 is a spherical lens of focal length f_2, and L_3 is a positive hemicylindrical lens of focal length f_3.

The cylindrical lenses are aligned with their cylindrical axes along the dispersion direction, so that they have no effect on images in the horizontal direction. The objective and image distances u and v of L_2 are determined by the usual formula $u^{-1} + v^{-1} = f_2^{-1}$ with u/v = reduction ratio. The cylindrical lenses are so spaced that focusing conditions are satisfied for both orthogonal directions. First assume that all lenses have negligible thickness. The following equations then relate the different lens parameters as defined in Fig. 2:

$$\begin{aligned} u^{-1} + v^{-1} &= f_2^{-1}; \\ u/v = k &= \text{reduction ratio}; \\ (u - T)^{-1} + h^{-1} &= f_1^{-1}, \ (f_1 < 0); \\ (h + T)^{-1} + g^{-1} &= f_2^{-1}; \\ g^{-1} + w^{-1} &= f_3^{-1}; \\ s + w &= v. \end{aligned} \tag{1}$$

These equations are solved with the following input parameters: u; f_1; T; f_2; and f_3. With a given reduction ratio u is fixed and the f's are all predetermined lens parameters. This leaves T as the only freely variable parameter. It turns out that the vertical reduction ratio is nearly independent of T, but depends on f_3, as shown in Fig. 3.

The ratio among the f's determines the optical characteristics of the system, while the magnitude of any of the f's determines the physical dimension of the system. In order to avoid impractically large transfer system or complex cylindrical optics configurations that pose fabrication problems, we chose for L_2 a *F*:2 50-mm

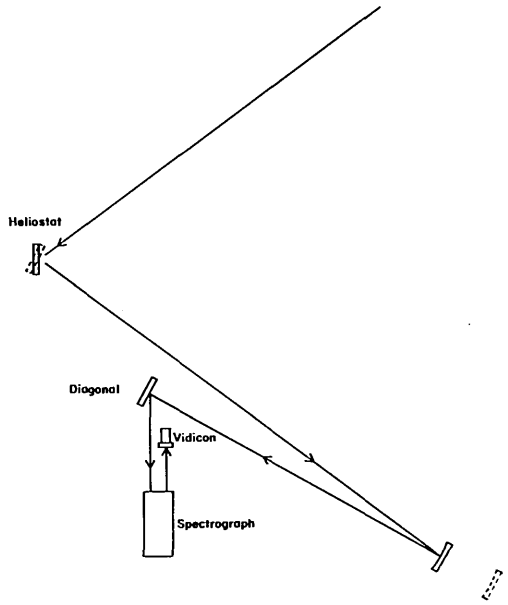

Fig. 1. Schematics of optical paths of the McMath telescope. The dotted positions are used for autocollimation for the introduction of calibrated light sources into the optical system.

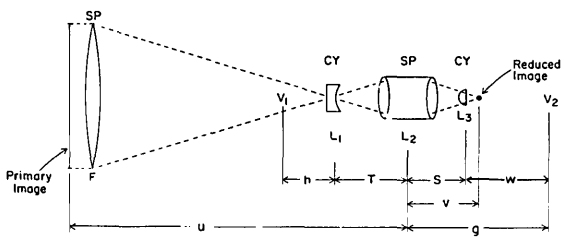

Fig. 2. Schematics of the anamorphic optical system described. Dispersion is in the direction perpendicular to the schematic. The primary image *PI* in the horizontal direction, uneffected by the cylindrical lenses, is imaged by L_2 to form the transferred image *RI* with objective distance u and image distance v as indicated. In the vertical direction, the primary image is reimaged by L_1 (negative cylindrical lens) to form a virtual image at V_1, which is then reimaged by L_2 to form a real image at V_2. L_3 brings the image at V_2 to *RI*.

Nikon lens (model HC) whose multilayer coating allows around 80% throughput transmission at wavelengths of interest (3900 Å) and whose linearity and resolution characteristics are quite satisfactory. Its moderate cost is another advantage. The strongly curved cylindrical lens L_3 represents a fabrication problem according to several optics manufacturers, and therefore we finally selected a hemispherical rod of 0.68-cm radius. The index of refraction of the glass is 1.67, and this gives a focal length of $R/(n-1) = 1.01$ cm. The combined vertical reduction ratio can be worked out to be between 36 and 42, depending on the final settings. Focusing is achieved by varying the distance between L_2 and L_3 via the focusing movement of the Nikon *F*:2 lens.

The strongly curved cylindrical lens L_3 has some cylindrical aberration associated with it. The best configuration is found to be the one with the flat side facing the image. The focal plane is, however, only 6 mm from the flat surface of the lens. A simple ray tracing calculation was programmed for the HP-65 electronic calculator for this configuration. It assumed parallel entrance rays which is not a bad approximation. We found that up to 75% of the linear aperture of the cylindrical lens can be used, while the defocused vertical image is no greater than the designed width of the vertical image. In actual usage, roughly only 50% of the linear aperture is used. Furthermore, if spectral features are aligned in the vertical direction, aberrations can only elongate the vertical image without sacrificing resolution in the dispersion direction. Figure 4 shows the calculated height of a point image as a function of the linear aperture.

V. Results of Tests at McMath Telescope

Tests of the complete system, including transfer optics, were accomplished at the photographic port of the McMath telescope vertical spectrograph.[5] The following tests were made:

(1) Cylindrical aberration. The transfer optics are rotated through 90° so that the scanning lines are nor-

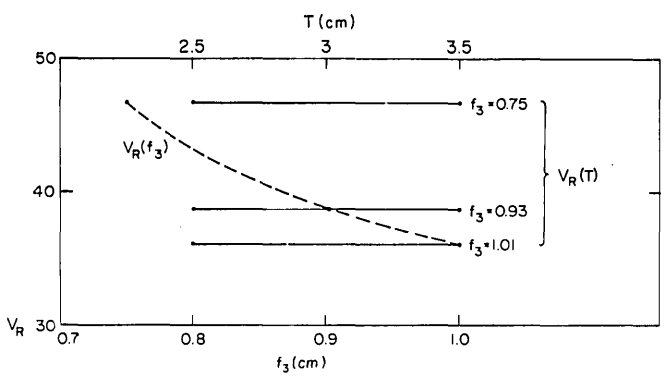

Fig. 3. The vertical reduction ratio V_R as a function of T and (see Fig. 2) and f_3.

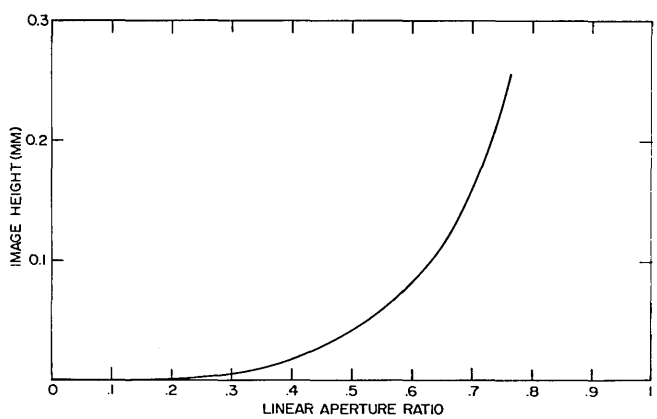

Fig. 4. The height of a point image as a function of the linear aperture ratio (fraction of hemispherical lens used in the vertical direction).

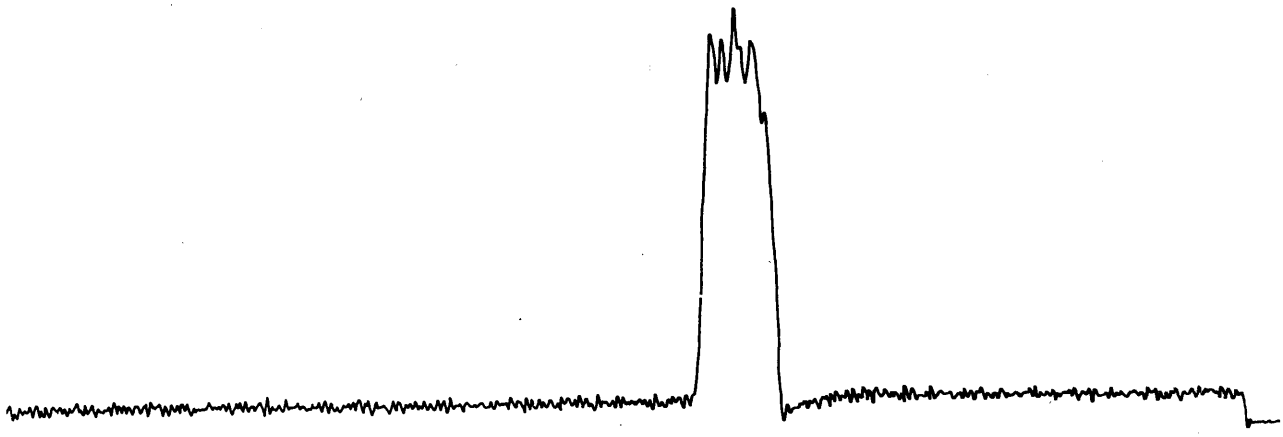

Fig. 5. The profile of the height of a spectrum. The total width is around 0.5 mm.

mal to the dispersion direction. A laser beam is autocollimated by the telescope and directed to the spectrograph, and the resulting spectrum is recorded. Figure 5 shows the profile of the height of spectrum. The irregularities at the peak of the profile corresponds to structural elements of the KPNO image slicer. The slight overshoot at one end of the profile simply reflects recording pen response.

Note that there is no detectable signal beyond the main profile. The fall of the profile on each wing is quite abrupt, reaching zero intensity within 5 pixels. This indicates that the cylindrical aberration is negligible.

(2) Resolution of the entire system. In this test, the transfer optics are oriented so that the scanning lines are parallel to the direction of dispersion. The spectrum of the laser with the telescope in autocollimation is again recorded. The spectral profile in terms of individual pixels is shown in Fig. 6. It is seen that the full width at half-maximum contains 4 to 5 pixels. A detailed analysis of the resolution, using solar spectrum and thorium spectrum, yields an over-all resolution of 55 mÅ of full width at half-maximum.[6] This is to be compared with the design resolution of 50 mÅ of the vertical spectrograph.[5]

(3) Actual observations of stellar and solar spectra. We have carried out a number of astronomical observations with this instrument. Results of these investigations are being published elsewhere.[6] Here we will illustrate the system performance by comparison of traces of single video scan lines to well established results of previous authors. Figure 7 shows a single-line video trace of the solar spectrum near the CN bandhead at 3883 Å, as obtained with the present system, compared with a photoelectric scan of the same spectral region, as obtained with the identical spectrograph and telescope. In our work, the spectrograph is used in single-pass mode (with a factor of 1000 attenuation), while the photoelectric scan was obtained in double-pass mode to eliminate scattered light.[7] Figure 8 shows a single line video trace of the CaII K line of the sun as

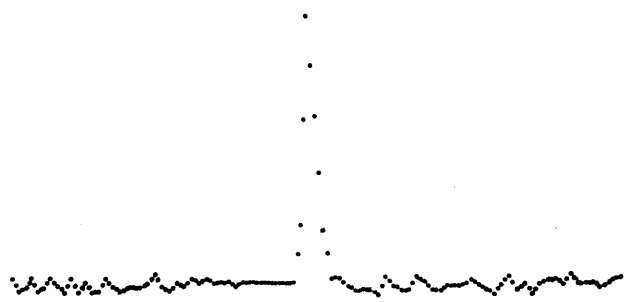

Fig. 6. The pixel-by-pixel spectrum of a laser obtained with our vidicon system at the McMath telescope.

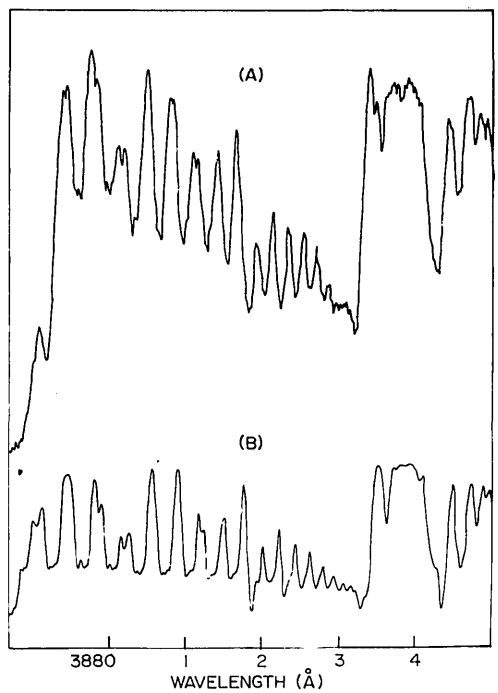

Fig. 7. A typical single line video trace of the solar spectrum near the CN bandhead at 3883 Å (A) as compared with that obtained with a photoelectric scan of the same spectral region, using a double pass mode (Kitt Peak Atlas) (B).[7] Note that there are around twelve to sixteen video traces in a spectrum in our system.

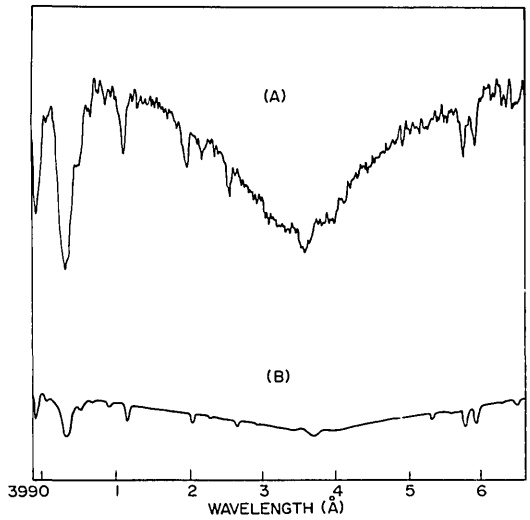

Fig. 8. Single video trace of the CaII K line of the sum (A) as compared to that from photoelectric scans (B).

compared to that from photoelectric scans. Figure 9 shows a single line video trace of the Ca II K line of the star Arcturus, with an exposure time of 15 min. The results of Griffin[8] in the same spectral region are shown for comparison. The exposure time reported by Griffin, using a 2.5 m (100-in.) telescope, was 159 min. Taking account of differences in apertures but not differences in spectrographs, the gain over using direct photography is around 31. In fact, the KPNO solar spectrograph, as used by us for stellar work, is rather slow (with a grating efficiency of only 4% in the seventh order as compared to certain echelle spectrographs where the efficiency may be as high as 50%).

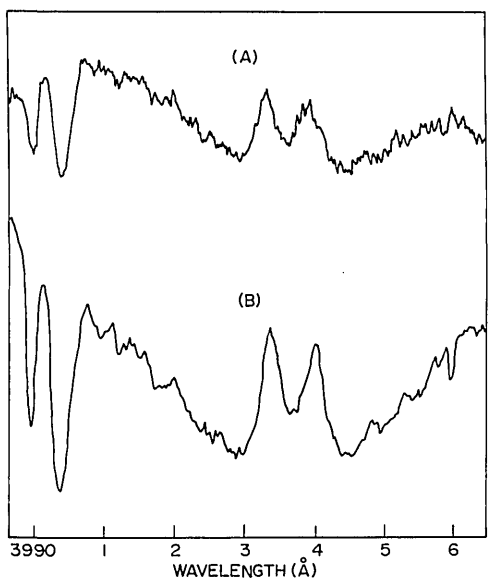

Fig. 9. Single video trance of the CaII K line of the star Arcturus (A) as compared with the spectrum obtained by Griffin[8] (B).

In all cases the TV data look more noisy than the photoelectric data. However, the TV data are single line video data. Since there are approximately sixteen video lines for the entire frame, when the entire frame is processed, the SNR is improved by roughly a factor of 4. Indeed, the processed data have approximately the same SNR as the photoelectric data.

VI. Discussions

Although SEC vidicons are capable of long exposure time, low light level integrations, we would like to point out some problems we encountered during the operation of our system.

Four limitations of the SEC vidicon have been cited: low target gain (~50); target grain noise; nonlinear response; and low target storage capacity (around 2000 photoelectrons per pixel). In our experience the problem of low target gain is now gradually overcome by improved electronic components and improved preamplifier designs, with a threshold of detection at about 10 photoelectrons per pixel. The target grain noise is usually comparable or less than the preamplifier noise (see below, however) and does not emerge conspicuously unless several frames are added together. Even then, it can be removed in data reduction process. Likewise, the nonlinear response can be removed by data processing and through proper calibration. The storage capacity problem can be solved by using external mass storage devices (such as disk memory). On the other hand we do find three problems which are associated with individual tubes. (Tube characteristics vary even among the same batch manufactured at the same time.)

(1) Microphonics. The resonance frequency of the target is around 1500 Hz for the WX 31958 tube and at a 60-Hz line-scanning frequency, a resonance is sometimes established, and some tubes are much more susceptible to microphonics than the others. This is exacerbated when the vidicon photocathode window is cooled by a directed stream of cold gas, or when mechanical vibrations are present in the environment. We have found, however, that if the readout is interrupted from line to line (e.g., when reading the output into a digital tape recorder) the microphonics tend to be damped.

The microphonics are caused by the excitation of the target and the mesh structures (which are made of magnetic materials) by the deflecting field, especially during the retrace portion of the scan. When the resonance frequency of the structures is close to the frequency of deflection, microphonics can be set up. However, by interrupting the deflection (when reading signals into a digital tape recorder), the oscillation may be damped since the disturbances are not pumped at a harmonic of the line period.

(2) Excessive target grain noise. Although in principle the target noise can be removed by data reduction, it is desirable that it be kept as small as possible. We have found, in a number of tubes, that when the target voltage exceeds 12 V, excessive noise (around two to three times the preamplifier noise) is present in areas

exposed to light. Reducing the target voltage to 10 V or lower tends to reduce the target noise. Some tubes do have less target noise.

(3) Dark count. For photocathodes composed of bialkali material with low red response, the dark noise is usually negligible for temperatures below 30°C. However, we have found that in the case of trialkali (S-20 photocathodes), the dark noise limits the exposure unless the photocathode is cooled to 0°C or below. Some tubes exhibit, after a number of hours of use, permanent discrete regions of the photocathode characterized by excessive dark noise that cannot be reduced by cooling.

In conclusion, we believe that within the limitations of the SEC vidicon, it is the only available video tube capable of high resolution in low light level integration apications with moderate cooling. The most serious problem, in our opinion, is the relative low yield of a good tube without the three problems cited above (at least the latter two). Practical experience in the vidicon industry cited a yield rate of only 10% for a quality tube. In view of the importance of low light level imagery, perhaps a concerted effort should be made to increase the yield of good tubes.

We thank S. P. Maran, R. W. Hobbs, and staff of the Laboratory for Solar Physics and Astrophysics, NASA Goddard Space Flight Center, for much encouragement and support, K. Schrubba for assistance in the construction, J. L. Linsky and G. S. Basri of JILA for participating in the observation program and discussions, P. J. Adams for setting up data analysis procedures, S. H. Chang for handling the data, J. L. Lowrance and P. Zucchino for much advice in vidicon technology and for reading the manuscript, and finally we thank Pius Nold and W. Whitson of the Westinghouse Corporation for their endless efforts to provide us with good SEC vidicon tubes.

References

1. G. W. Goetze and A. H. Boerio, Proc. IEEE **52,** 1007 (1964).
2. A. H. Boerio, R. R. Beyer, and G. W. Goetze, Adv. Electron. Electron Phys. **22A,** 229 (1966); G. W. Goetz, Adv. Electron. Electron Phys. **22A,** 219 (1966).
3. P. Zucchino and J. L. Lowrance, Adv. Electron. Electron Phys. **28A,** 851 (1973).
4. P. Zucchino and J. L. Lowrance, "Progress Report on Development of the SEC-vidicon for Astronomy," in *Astronomical Use of Television Type Sensors, Symposium Proceedings, Princeton Observatory, 20, 21 May 1970,* NASA SP-256 (1971), pp. 27–53. P. Zucchino, Adv. Electron. Electron Phys., in press.
5. A. K. Pierce, Appl. Opt. **3,** 1337 (1964).
6. H. Y. Chiu, P. S. Adams, J. L. Linsky, G. S. Basri, S. P. Maran, and R. W. Hobbs, Astrophys. J., Dec. 15 (1976).
7. J. Brault and L. Testerman, *Kitt Peak Wavelength Atlas* (Kitt Peak National Observatory, Tucson, Ariz., 1972).
8. R. F. Griffin, *A Photometric Atlas of the Spectrum of Arcturus* (Cambridge Philosophical Society, Cambridge, 1968).

SECOND EUROPEAN OPTICS SUMMER SCHOOL

Following the success of the European Optics Summer School held at the University of Reading, England, in 1975, under ICO sponsorship, it has been decided to hold a similar school in 1977. The dates will be July 18 to July 29,1977, and H.H. Hopkins will again be Course Director.